

Grating visual acuity impairment assessed by sweep visually evoked potentials in children with optic pathway tumors unable to perform optotype acuity tests

Deficiência na acuidade visual de grades avaliada pelos potenciais visuais evocados de varredura em crianças com tumores da via óptica incapazes de informar a acuidade de optotipos

Patrícia de Freitas Dotto¹ , Adriana Berezovsky¹ , Andrea Maria Cappellano², Nasjla Saba da Silva², Paula Yuri Sacai¹ , Daniel Martins Rocha¹, Erica Pinheiro de Andrade¹ , Frederico Adolfo B. Silva², Solange Rios Salomão¹

1. Laboratório de Eletrofisiologia Visual Clínica, Departamento de Oftalmologia e Ciências Visuais, Escola Paulista de Medicina, Universidade Federal de São Paulo, São Paulo, SP, Brazil.

2. Programa de Neuro-Oncologia, Instituto de Oncologia Pediátrica, Grupo de Apoio ao Adolescente e à Criança com Câncer, Universidade Federal de São Paulo, São Paulo, SP, Brazil.

ABSTRACT | Purpose: To determine visual impairment due to optic pathway tumors in children unable to perform recognition acuity tests. **Methods:** Grating visual acuity scores, in logMAR, were obtained by sweep visually evoked potentials (SVEP) in children with optic pathway tumors. The binocular grating visual acuity deficit was calculated by comparison with age-based norms and then assigned to categories of visual impairment as mild (from 0.10 to 0.39 logMAR), moderate (from 0.40 to 0.79 logMAR), or severe (≥ 0.80 logMAR). Interocular differences were calculated by subtraction and considered increased if > 0.10 logMAR. **Results:** The participants were 25 children (13 boys; mean \pm SD age, 35.1 ± 25.9 months; median age, 32.0 months) with optic pathway tumors (24 gliomas and 1 embryonal tumor), mostly located at the hypothalamic-chiasmatic transition ($n=21$; 84.0%) with visual abnormalities reported by parents ($n=17$; 68.0%). The mean grating acuity deficit was 0.60 ± 0.36 logMAR (median, 0.56 logMAR). Visual impairment was detected in all cases and was classified as mild in 10 (40.0%), moderate in 8 (32.0%), and severe in 7 (28.0%) children, along with increased interocular differences (> 0.1 logMAR) ($n=16$; 64.0%). The remarkable ophthalmological abnormalities were nystagmus ($n=17$; 68.0%), optic disc cupping and/or pallor ($n=13$; 52.0%), strabismus ($n=12$; 48.0%), and poor visual behavior ($n=9$; 36.0%). **Conclusion:** In children with optic pathway tumors who were unable to perform recognition

acuity tests, it was possible to quantify visual impairment by sweep-visually evoked potentials and to evaluate interocular differences in acuity. The severity of age-based grating visual acuity deficit and interocular differences was in accordance with ophthalmological abnormalities and neuroimaging results. Grating visual acuity deficit is useful for characterizing visual status in children with optic pathway tumors and for supporting neuro-oncologic management.

Keywords: Visual disorders; Evoked potentials, visual; Visual acuity; Visual pathways; Optic nerve glioma; Child

RESUMO | Objetivo: Determinar o grau de deficiência visual em crianças com tumores da via óptica incapazes de informar a acuidade visual de reconhecimento. **Método:** A acuidade visual de grades, em logMAR, foi estimada por potenciais visuais evocados de varredura em crianças com tumores das vias ópticas. O déficit da acuidade visual de grades binocular foi calculado em relação ao valor mediano normativo esperado para a idade e a deficiência visual, classificada como leve (0,10 a 0,39 logMAR), moderada (0,40 a 0,79 logMAR) ou grave ($\geq 0,80$ logMAR). Diferenças inter-oculares foram calculadas por subtração e consideradas aumentadas se $> 0,10$ logMAR. **Resultados:** Foram avaliadas 25 crianças (13 meninos; média de idade \pm DP = $35,1 \pm 25,9$ meses; mediana = 32,0 meses) com tumores da via óptica (24 gliomas e 1 tumor embrionário) localizados particularmente na transição hipotalâmico-quiasmática ($n=21$; 84,0%) e com anormalidades visuais detectadas pelos pais ($n=17$; 68,0%). A média do déficit da acuidade de grades foi $0,60 \pm 0,36$ logMAR (mediana = 0,56 logMAR). Observou-se deficiência visual leve em 10 (40,0%), moderada em 8 (32,0%) e grave em 7 (28,0%), além de aumento da diferença interocular da acuidade visual ($n=16$; 64,0%). As principais alterações oftalmológicas encontradas foram: nistagmo ($n=17$; 68,0%),

Submitted for publication: July 18, 2019
Accepted for publication: February 4, 2020

Disclosure of potential conflicts of interest: None of the authors have any potential conflicts of interest to disclose.

Corresponding author: Patrícia de Freitas Dotto Quaresma.
E-mail: patdotto@gmail.com

Approved by the following research ethics committee: Universidade Federal de São Paulo UNIFESP/EPM (CAAE 30972314.0.0000.5505).

aumento da escavação do disco óptico e/ou palidez (n=13; 52,0%), estrabismo (n=12; 48,0%) e comportamento visual pobre (n=9; 36,0%). **Conclusão:** Em crianças com tumor da via óptica e incapazes de responder aos testes de acuidade visual de reconhecimento, foi possível quantificar deficiência visual por meio dos potenciais visuais evocados de varredura e avaliar a diferença interocular da acuidade visual de grades. A gravidade do déficit da acuidade visual de grades relacionado à idade e a diferença interocular da acuidade visual de grades foram congruentes com alterações oftalmológicas e neuroimagem. O déficit da acuidade visual de grades foi útil à caracterização do estado visual em crianças com tumores da via óptica e ao embasamento da assistência neuro-oncológica.

Descritores: Transtornos da visão; Potenciais evocados visuais; Acuidade visual; Vias visuais; Glioma do nervo óptico; Criança

INTRODUCTION

Brain tumors are common space-occupying pediatric neoplasms, with an incidence varying from 1.12 to 5.14/100,000 according to age range, histologic subtype, and country^(1,2). According to the Central Brain Tumor Registry of the United States statistical report, gliomas followed by embryonal tumors are prevalent in patients under 14 years old, whereas older patients usually present with pineal tumors followed by gliomas⁽³⁾. Activation and overexpression of proto-oncogenes, as well as loss or inactivation of tumor suppressor genes, are the main biological mechanisms underlying the neoplastic changes⁽⁴⁾. In the course of disease development, several neuronal routes can be disrupted. Vision may be progressively disturbed by optic pathway compression, tumor invasion, or even surgical intervention^(5,6), leading to irreversible blindness, considered as one of the most dramatic neurological sequelae in survivors⁽⁷⁾.

Because the visual system in children is still developing, even temporary interruption of normal visual input can lead to a permanent decrease in vision from amblyopia⁽⁸⁾. Mild visual disturbances may be hardly recognizable or misinterpreted as benign ophthalmic morbidities, delaying the diagnosis in small children⁽⁹⁾.

Visual acuity (VA) testing using optotypes such as Snellen charts, Early Treatment Diabetic Retinopathy Study (ETDRS) charts, or Lea symbols is usually the gold standard for assessment of visual function in children with brain tumors⁽¹⁰⁾. These tests evaluate recognition acuity, which is the ability to recognize and name symbols (optotypes) presented in table form or designed, built on the principles of Snellen. The optotypes must be larger than the detection limit of the subject. A limitation

of the method is that it is difficult to apply in preverbal, uncooperative, or cognitively impaired children who are unable to perform recognition tasks⁽¹¹⁾. Therefore, alternative methods for visual function assessment may be required⁽¹²⁻¹⁴⁾.

An alternative method of evaluating VA is the adoption of resolution acuity techniques. Resolution acuity is measured by the smallest angle of separation between critical elements of a standardized stimulus composed of pairs of points, grids, or chess patterns that an individual can discriminate. Resolution acuity, such as grating acuity, can be measured subjectively by Teller acuity cards or objectively by the sweep visually evoked potentials (SVEP) technique^(12,13). Both techniques have been clinically used in recent decades as ancillary tests to evaluate subjects who are unable to perform recognition VA. The advantages of SVEP are that it provides an objective, reliable, and rapid (requiring only a 10-second trial) estimation of VA. It has become a precise method of evaluating uncooperative children⁽¹⁴⁾. Moreover, SVEP is based on cortical threshold responses, which reduces the influence of the examiner on VA results.

Although SVEP has been employed to monitor VA during normal development⁽¹³⁾ and in severe clinical conditions associated with blindness^(15,16), few studies have employed SVEP to investigate visual function in patients with brain tumors^(17,18). Obtaining reliable data on visual function from a sick child with a brain tumor is difficult, but maximizing this information can influence future treatment decisions⁽¹⁹⁾.

The purpose of this study was to determine grating visual acuity deficits (GVAD) and visual impairment in children with optic pathway tumors who were unable to undergo recognition acuity testing due to young age, developmental delay, or neurological sequelae. We believe our results can provide useful information to hasten suspected diagnoses and neuro-oncologic management, aiming to achieve optimal visual outcomes in survivors.

METHODS

Children diagnosed with optic pathway tumors were referred to the Clinical Electrophysiology of Vision Laboratory of the Universidade Federal de São Paulo (UNIFESP) for grating acuity measurement by SVEP between May 2002 and May 2018. The study followed the tenets of the Declaration of Helsinki and its later amendments. Institutional Review Board approval was obtained from the Committee on Ethics in Research of UNIFESP.

The inclusion criteria were children 8 years old or younger, unable to perform recognition VA testing, with an unequivocal diagnosis of optic pathway tumors determined by pediatric neuro-oncology experts and classified according to the 2016 World Health Organization Classification of Tumors of the Central Nervous System⁽¹⁹⁾. The exclusion criteria were infectious diseases, congenital or drug-induced cataract, structural abnormalities affecting the visual axis, and abnormal macular aspect.

Ophthalmic assessment of children with optic pathway tumors included visual fixation, visual pursuit, eye alignment (Hirschberg, Krimsky, or cover test), presence of nystagmus, external examination of the eyes, and fundus examination. All children were awake, alert, and wearing their glasses when required. Symptoms, tumor onset, tumor location on neuroimaging, and tumor management were also noted.

Binocular and monocular grating visual acuity (GVA) measurements were performed using the PowerDiva (digital infant vision assessment) SVEP system (Smith-Kettlewell Eye Research Institute, San Francisco, CA, USA)⁽¹⁴⁾. The SVEP system is composed of two interfacing Macintosh G3 computers: the “host” computer, in charge of stimulus trial parameters and analysis of visually evoked potentials (VEP), and the “video” computer, linked to the monitor where stimuli are shown to the subject. The SVEP procedure was performed in a dark room with the child seated on their parent’s lap or in a wheelchair. SVEP was recorded only when the subject was alert and fixating the stimuli. To ensure attention, small toys were dangled over the center of the display. The total testing time, including setup and rest breaks, typically lasted from 10 to 30 minutes, depending on the subject’s age and cooperation.

The electroencephalogram (EEG) was recorded from two bipolar active placements (O_1 and O_2) with a ground electrode positioned 1 cm above the inion on the midline (O_z), in accordance with the 10-20 System. A reference electrode was placed on the vertex (C_z). Electrodes (Grass Gold Disc Electrodes-E6GH, Astro-Med Inc. USA) were attached to the scalp with electrode cream after cleansing the scalp with abrasive paste and cotton pads. A headband (3M Coban self-adherent Wrap 1581) was used to keep the electrodes in place. The stimuli were phase-reversal sine-wave gratings presented on a high-resolution 17-inch monochromatic video monitor (M20DCD4RE-Richardson Electronics® Ltd. USA) at a fixed contrast (80%) and mean luminance of 142.35 cd/m².

The test stimulation field varied from 52° × 65° (for 30-cm distance) to 11° × 14° (for 150-cm distance), for both vertical and horizontal monitor lengths. For all tests, the spatial frequency was swept (from 0.1 to 30 cycles per degree) by the viewing distance (30 to 150 cm) with temporal modulation of 6.6 Hz. Ten linearly spaced spatial frequencies were presented at a rate of 1/s, starting at a low spatial frequency. The gratings were vertically oriented, except in cases of horizontal nystagmus⁽¹³⁻¹⁶⁾.

The recordings were adaptively filtered (bandpass) in real time (sampling rate, 397 Hz) to isolate the VEP. The potential differences were amplified (Neurodata Acquisition System P15, Grass Instrument Co., USA) (gain, 10,000; - 3 db cutoff at 1 and 100 Hz). Three to 15 repetitions of the sweep were obtained and vector averaged. The amplitude and phase of the first (6 Hz) and second (12 Hz) harmonics of the stimulus frequency were calculated for each channel by discrete Fourier transform⁽¹³⁻¹⁶⁾.

Grating acuity was estimated with an automated algorithm that performed a linear fit and extrapolation to zero amplitude for the final descending limb of the function relating each VEP amplitude (from the second harmonic) to a linear spatial frequency (Figure 1). A signal-to-noise ratio (SNR) at a peak of 3:1 was required and calculated as the ratio of the power at stimulus frequency to the mean power at frequencies ± 2 Hz, corresponding to a false alarm rate of 0.4 %, ensuring an adequate protection level when combined with the phase consistency criteria. In all cases, two thresholds (one for O_1 and another for O_2) were obtained. The final acuity score was calculated in logMAR (logarithm of the minimum angle of resolution) using the results in cycles per degree of visual angle of the better threshold channel with the highest SNR⁽¹³⁻¹⁶⁾.

The eye with the better grating acuity measurement was classified as the better-seeing eye (BSE) and the fellow eye as the worse-seeing eye (WSE). If similar acuities were found in both eyes, the BSE was randomly assigned using the RANDARRAY function of MExcel Software considering 0 as the right eye and 1 as the left eye. Visual acuities of light perception (previously confirmed by transient flash visually evoked potentials recordings) were assigned as 3.0 logMAR⁽⁵⁾. Monocular measures were employed to calculate interocular acuity differences (IAD) by subtraction; the IAD was classified as increased if >0.1 logMAR.

Binocular GVAD was obtained by subtracting binocular GVA scores from the age-related median norm⁽¹⁴⁾.

Visual impairment was categorized as mild ($0.39 \geq \text{GVAD} \geq 0.10 \text{ logMAR}$), moderate ($0.79 \geq \text{GVAD} \geq 0.40 \text{ logMAR}$), or severe ($\text{GVAD} \geq 0.80 \text{ logMAR}$)⁽¹⁵⁾. To validate the method, the cutoff value of 0.10 logMAR in GVAD for normal acuity was previously established as a function of GVA variation from a group of 10 healthy children aged 8 years or younger (6 girls; mean \pm SD age, 75.0 \pm 15.6 months; median age, 76.0 months), presenting with recognition VA equal to 0.00 logMAR (20/20 Snellen fraction) and normal ophthalmological examination (normal fundus, normal ocular motility, normal Titmus stereo test equal to 40", preserved pupillary reflexes,

best-corrected VA 4-m ETDRS chart equal to or better than zero logMAR, and spherical equivalent of the refractive status from - 6.00 to + 6.00 diopters). In this control group, the monocular mean GVAs were $0.04 \pm 0.02 \text{ logMAR}$ (median, 0.04 logMAR) and $0.05 \pm 0.03 \text{ logMAR}$ (median, 0.06 logMAR) for BSEs and WSEs, respectively (Table 1).

Statistical analysis

An unpaired *t*-test was performed to compare GVAD between boys and girls with optic pathway tumors after the normality test (Shapiro-Wilks). The correlation between the age of tumor onset and GVAD was investigated by the Pearson correlation test. Statistical significance was established at $p \leq 0.05$.

RESULTS

The participants were 25 children (13 boys) with ages ranging from 3 to 95 months (mean \pm SD, 35.1 \pm 25.9 months; median, 32.0 months), with optic pathway tumors and unable to perform recognition acuity tests. The age of tumor onset ranged from birth to 36 months (mean \pm SD, 10.8 \pm 11.3 months; median, 6.0 months). The lesions were classified as diffuse astrocytic and oligodendroglial tumors (n=13), including 6 low-grade gliomas, 6 astrocytomas, and 1 glioblastoma; other astrocytic tumors (n=10), including 9 pilocytic

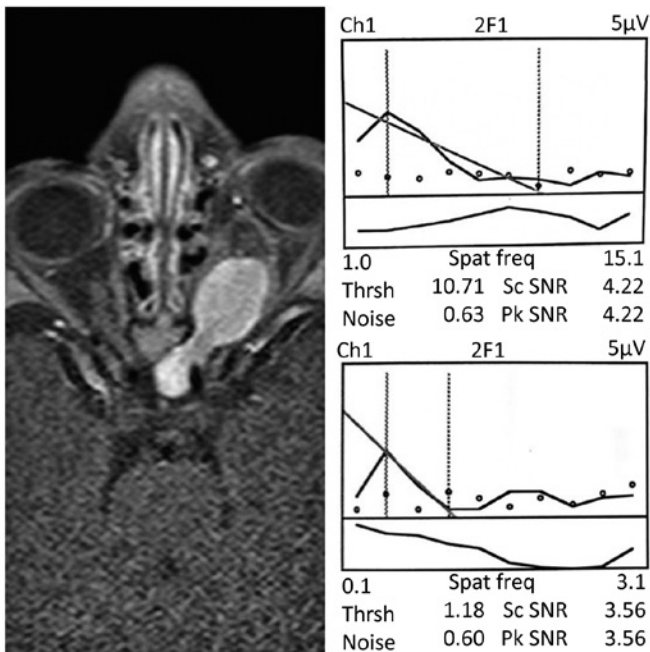


Figure 1. Representative sweep visually evoked potential (SVEP) response from the better-seeing eye (BSE) and the worse-seeing eye (WSE) (right panel) and orbital magnetic resonance imaging (MRI) (left panel) from subject S01. Right panel: SVEP from channel 1 (O1-Cz). Dots represent noise registered for each of 10 linearly spaced spatial frequencies presented (from 1.00 to 15.10 cycles/degree presented at 80 cm for the right eye and from 0.1 to 3.01 cycles/degree presented at 30 cm for the left eye); grating acuity was estimated by linear fit and extrapolation to zero amplitude, i.e., the value at which the regression line touches the axis of spatial frequencies; the final acuity scores were thresholds of 10.71 cycles/degree, equal to 0.44 logMAR (or 20/55 Snellen fraction) for the BSE and 1.18 cycles/degree, equal to 1.40 logMAR (or 20/510). The signal-to-noise ratio was 4.22 for the right eye and 3.56 for the left eye. Left panel: Enhanced axial T1-weighted MRI (960/20 [repetition time msec/echo time msec]) shows high signal intensity around the left optic nerve from its intraorbital portion to the chiasm, whereas the intraorbital portion of the right optic nerve is normal. The reduced grating visual acuity (GVA) in the right eye (BSE) is probably due to effects on the optic nerve at the chiasm level. Abbreviations: Ch= channel; 2F1s= harmonic of the stimulus frequency; Spat Freq= spatial frequency; Thrsh= grating acuity threshold (cycles/degree); SNR= signal-to-noise ratio; Sc SNR= maximum SNR within the cursors (dotted lines) that define the data used to estimate threshold; Pk SNR= maximum SNR at peak mean amplitude in the record.

Table 1. Demographics, recognition (Snellen optotypes), and grating visual acuity (GVA) measured by the sweep visually evoked potentials (SVEP) technique, both expressed in the logarithm of the minimum angle of resolution (logMAR), and the spherical equivalent of the refractive error, in diopters (D), from the better-seeing eyes (BSE) and the worse-seeing eyes (WSE) of 10 healthy children

Individual	Sex/age (mo)	BSE		WSE	
		Snellen optotypes (logMAR)	GVA (logMAR)	Snellen optotypes (logMAR)	GVA (logMAR)
C01	F/52	0.00	0.03	0.00	0.04
C02	F/55	0.00	0.02	0.00	0.06
C03	M/60	0.00	0.04	0.00	0.05
C04	M/70	0.00	0.01	0.00	0.01
C05	F/72	0.00	0.05	0.00	0.06
C06	F/80	0.00	0.01	0.00	0.03
C07	F/85	0.00	0.01	0.00	0.01
C08	M/88	0.00	0.06	0.00	0.08
C09	F/93	0.00	0.06	0.00	0.07
C10	M/95	0.00	0.07	0.00	0.09

astrocytomas and 1 pilomyxoid astrocytoma; neuronal and mixed neuronal-glial tumors (n=1): 1 desmoplastic infantile ganglioglioma and embryonal tumors (n=1): 1 atypical teratoid/rhabdoid tumor.

Optic pathways were affected in all patients, mainly at the hypothalamic-chiasmatic transition (n=21; 84.0%). The mechanism of optic pathway disturbance by tumors was inward growth in 11 children (44.0%), secondary compression by raised intracranial pressure or mass effect in 9 children (36.0%), and both mechanisms in 5 children (20.0%). Oncologic management varied as a function of tumor type and location, requiring both single and combined therapies, including observation, chemotherapy, and/or tumor resection, and associa-

ted procedures, such as ventriculoperitoneal shunting (VPS), autologous bone marrow transplantation, and external radiation therapy. A complete description of each case, including tumor type, tumor location, effects of the tumor on the visual system, and treatment, can be found in table 2. Ocular findings and VA measurements for each participant are described in table 3.

Visual abnormalities at diagnosis were reported by parents in 17 children (68.0%) and included shaking eyes (n=12), eye misalignment (n=2), proptosis (n=1), and ptosis (n=1). At SVEP evaluation, nystagmus (n=17; 68.0%), optic disc cupping and/or pallor (n=13; 52.0%), strabismus (n=12; 48.0%), and poor visual behavior (n=9; 36.0%) were observed.

Table 2. Demographics, tumor type, tumor location, suspected mechanism of effect on optic pathway, and treatment of 25 children with optic pathway tumors according to visual impairment category

Patient	Sex	Age (mo)	Tumor onset (mo)	Tumor type	Tumor location	Tumor effect on visual system	Treatment
Mild visual impairment (n=10)							
S01	M	12	3	Astrocytoma	Hypothalamic/chiasmatic	Inward growth	Chemotherapy
S02	M	13	0	Pilocytic astrocytoma	Hypothalamic/chiasmatic	Mass effect	Chemotherapy + resection
S03	F	15	3	Pilocytic astrocytoma	Optic tract (left)	Inward growth	Observation
S04	F	32	0	Glioblastoma	Occipital lobe	Inward growth	Chemotherapy + resection
S05	M	43	31	Astrocytoma	Hypothalamic/chiasmatic	Inward growth	Observation
S06	F	50	36	Low-grade glioma	Hypothalamic/chiasmatic	Inward growth + raised ICP	Chemotherapy + VPS
S07	F	65	12	Pilocytic astrocytoma	Hypothalamic/chiasmatic	Inward growth + raised ICP	Chemotherapy + VPS
S08	M	79	24	Pilocytic astrocytoma	Hypothalamic/chiasmatic	Mass effect + raised ICP	Resection + VPS
S09	M	94	4	Astrocytoma	Hypothalamic/chiasmatic	Mass effect + raised ICP	Chemotherapy + resection + VPS
S10	M	95	36	Low-grade glioma	Hypothalamic/chiasmatic	Inward growth	Observation
Moderate visual impairment (n=8)							
S11	M	3	1	Teratoid/rhabdoid	Hypothalamic/chiasmatic	Mass effect	Resection
S12	F	8	5	Pilocytic astrocytoma	Hypothalamic/chiasmatic	Inward growth + raised ICP	Chemotherapy + VPS
S13	F	9	0	Low-grade glioma	Hypothalamic/chiasmatic	Inward growth	Observation
S14	F	10	6	Pilocytic astrocytoma	Hypothalamic/chiasmatic	Inward growth	Chemotherapy
S15	F	17	6	Astrocytoma	Hypothalamic/chiasmatic	Mass effect + raised ICP	Chemotherapy + resection
S16	F	36	6	Low-grade glioma	Hypothalamic/chiasmatic	Inward growth	Chemotherapy
S17	F	40	5	Astrocytoma	Hypothalamic/chiasmatic	Inward growth	Chemotherapy + EVP
S18	M	54	21	Pilocytic astrocytoma	Hypothalamic/chiasmatic	Mass effect + raised ICP	Chemotherapy + resection + VPS
Severe visual impairment (n=7)							
S19	F	18	6	Low-grade glioma	Hypothalamic/chiasmatic	Inward growth + raised ICP	Chemotherapy + VPS
S20	M	20	14	Pilocytic astrocytoma	Hypothalamic/chiasmatic	Mass effect	Chemotherapy + resection
S21	M	26	6	Desmoplastic infantile ganglioglioma	Occipital lobe	Mass effect	Resection
S22	F	26	22	Pilocytic astrocytoma	Hypothalamic/chiasmatic	Inward growth + raised ICP	Chemotherapy + VPS
S23	M	33	6	Low-grade glioma	Hypothalamic/chiasmatic	Inward growth	Chemotherapy
S24	M	37	18	Astrocytoma	Hypothalamic/chiasmatic	Mass effect + raised ICP	Chemotherapy + resection + VPS
S25	M	42	0	Pilomyxoid astrocytoma	Lateral geniculate body (right)	Inward growth	Resection

ICP= intracranial pressure; VPS= ventriculoperitoneal shunting.

Table 3. Demographics, clinical features, grating visual acuity (GVA) scores, and visual deficits in 25 children with optic pathway tumors according to visual impairment category

Patient	Sex/age (mo)	Clinical presentation	Seizures	Ocular motility and nystagmus	Fundus	GVA OU (logMAR)	GVA deficit (logMAR)	GVA BSE (logMAR)	GVA WSE (logMAR)	IAD (logMAR)
Mild visual impairment (n=10)										
S01	M/12	Proptosis	No	XT LE	Cupping WSE	0.44	0.11	0.44	1.40	0.96
S02	M/13	NF1 and shaking eyes	No	ORTHO/Nys	NA	0.63	0.30	0.61	0.63	0.02
S03	F/15	Ptosis	No	ORTHO	Normal OU	0.71	0.38	0.71	3.00	2.29
S04	F/32	Bulging fontanelle	Yes	XT LE	Normal OU	0.40	0.29	0.39	0.53	0.14
S05	M/43	NF1 and shaking eyes	No	ORTHO	Normal OU	0.35	0.30	0.35	0.40	0.05
S06	F/50	Vomiting and shaking eyes	No	ORTHO	Pallor OU	0.17	0.12	0.16	1.45	1.29
S07	F/65	Weight loss	No	XT LE	Normal OU	0.22	0.17	0.22	0.98	0.76
S08	M/79	Eye misalignment	No	XT RE	Pallor WSE	0.43	0.38	0.43	3.00	2.57
S09	M/94	NF1 and shaking eyes	Yes	XT OD/Nys	Pallor OU	0.39	0.34	0.47	0.55	0.08
S10	M/95	Vomiting and ptosis	No	ORTHO	Normal OU	0.24	0.19	0.26	0.66	0.40
Moderate visual impairment (n=8)										
S11	M/3	Vomiting and eye misalignment	No	XT	Normal OU	1.21	0.57	1.19	1.20	0.01
S12	F/8	Shaking eyes	Yes	ORTHO/Nys	Normal OU	0.93	0.56	0.93	3.00	2.07
S13	F/9	Shaking eyes	No	ORTHO/Nys	Cupping OU	0.91	0.54	0.44	0.95	0.51
S14	F/10	Shaking eyes	Yes	ORTHO/Nys	Cupping OU	0.79	0.42	0.93	0.93	0.00
S15	F/17	Shaking eyes	No	ORTHO/Nys	Pallor OU	0.84	0.66	1.09	1.25	0.14
S16	F/36	Shaking eyes	No	ORTHO/Nys	Normal OU	0.70	0.65	0.71	0.75	0.04
S17	F/40	Shaking eyes	No	ORTHO/Nys	NA	0.80	0.75	0.80	3.00	2.80
S18	M/54	Vomiting	No	XT RE	Cupping OU	0.65	0.60	0.65	1.15	0.50
Severe visual impairment (n=7)										
S19	F/18	Weight loss and eye misalignment	Yes	XT RE	Cupping OU	1.30	1.12	1.42	3.00	1.58
S20	M/20	Shaking eyes	No	ORTHO/Nys	Pallor OU	1.00	0.82	1.03	1.04	0.01
S21	M/26	Hypotonia	No	XT	Normal OU	1.31	1.17	1.31	1.37	0.06
S22	F/26	Eye misalignment	Yes	ET/Nys	Pallor OU	1.16	1.02	1.17	1.27	0.10
S23	M/33	Shaking eyes	No	XT LE/Nys	Pallor OU	1.04	0.93	1.04	3.00	1.96
S24	M/37	Shaking eyes	Yes	ET/Nys	Pallor OU	1.14	1.09	1.14	3.00	1.86
S25	M/42	Vomiting	No	ORTHO/Nys	Normal OU	1.50	1.45	1.50	3.00	1.50

IAD= interocular acuity difference; BSE= better-seeing eye; ET= esotropia; LE= left eye; NF1= neurofibromatosis type 1; Nys= nystagmus; OU= both eyes; RE= right eye; XT= exotropia; WSE= worse-seeing eye.
IAD >0.10 logMAR are shown in bold.

Visual impairment based on binocular GVAD (mean \pm SD, 0.60 ± 0.36 logMAR; median, 0.56 logMAR) was detected in all children and was classified as mild in 10 children (40.0%), moderate in 8 children (32.0%), and severe in 7 children (28.0%). Increased IAD (>0.1 logMAR) was found in 16 children (64.0%). GVAD was comparable in boys and girls, and no correlation was found between age at tumor onset and GVAD. A representative SVEP response from the BSE and the WSE and the orbital magnetic resonance imaging (MRI) from a participant (subject S01) are shown in figure 1. The binocular GVAD scores, in logMAR units, of each participant in compa-

ison with age norms from our laboratory are shown in figure 2. The distribution of all participants, considering the World Health Organization (WHO) classification of tumors, age (months) at SVEP evaluation, and GVAD scores (in logMAR units), is shown in figure 3.

DISCUSSION

Visual impairment was determined in a group of young children with hypothalamic-chiasmatic tumors who were unable to perform recognition VA tests. Age-based grating acuity deficits and interocular acuity

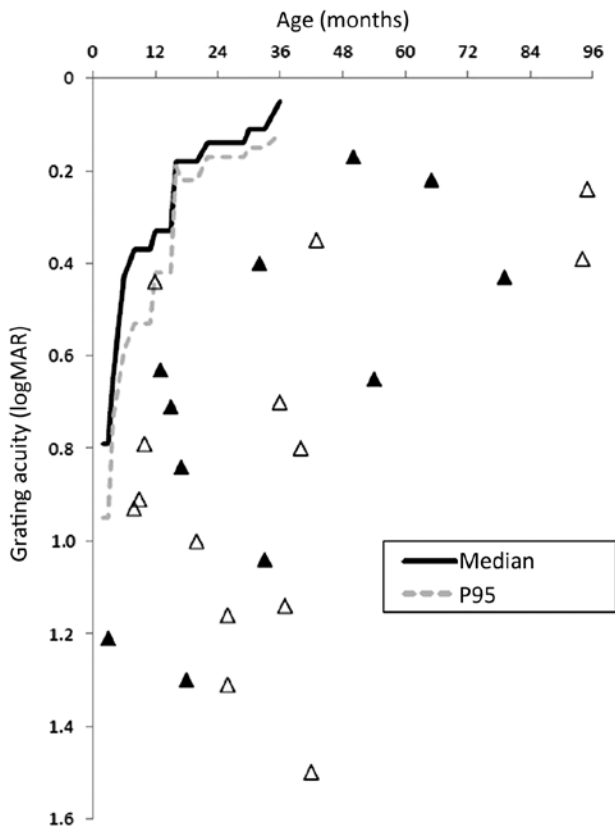


Figure 2. Binocular grating visual acuity scores (in logMAR units) from 25 children with optic pathway tumors compared with age norms from our own laboratory. Boys are represented by black triangles.

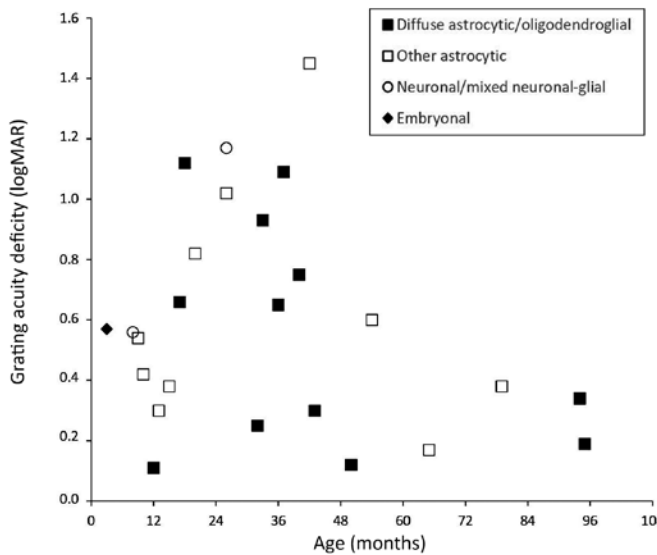


Figure 3. Distribution of 25 children with optic pathway tumors considering World Health Organization classification⁽¹⁹⁾, age at sweep visually evoked potential (SVEP) evaluation (in months), and binocular grating acuity scores (in logMAR units).

differences were in line with ophthalmological features and neuroimaging and demonstrated the negative impact of tumor lesions on visual status in all participants. Structural damage to the optic pathway was attributed to inward tumor growth and/or secondary compression by raised intracranial pressure.

A limitation of this study is that the majority of the children had been referred to our emergency service with serious life-threatening clinical conditions, preventing grating acuity measurement before oncologic management.

An important aspect to be considered when dealing with neuropediatric disorders affecting the visual pathway is the critical period of visual cortical development, occurring between birth and approximately 8 years of age^(12,13). During this specific window, uninhibited visual inputs from each eye are essential for the development of both monocular- and binocular-driven cells in the occipital lobe. Abnormal visual input or disuse of an eye can lead to decreased vision, which should be treated to prevent permanently affected vision⁽⁸⁾. Increased interocular acuity differences were observed in 16 of 25 children (64%), including 8 of 12 children with strabismus. According to clinical data (Table 3), eight children with strabismus presented with increased IAD, but only three of them (S01, S08, and S19) had noticeable eye misalignment on tumor diagnosis. Overall, strabismus was reported in the remainder of strabismic children (n=9/12) during follow-up. Thus, in our sample of children affected by optic pathway tumors during the critical period, grating acuity deficits and increased IAD highlight the deleterious impact of optic pathway tumors on vision and binocular interaction, as suggested by ocular motility disturbances.

The proportion of visual disturbances in the current series (Table 4) was similar to those observed in previous reports^(2,6,7,10,21-29). Optic disc abnormalities were attributed to axonal losses, whereas strabismus indicated oculomotor pathway disruption or cranial nerve palsies^(8,16). Reduced VA may be explained by abnormal information processing in early visual areas⁽¹⁶⁾, pre-existing damage in the visual system, and tumor growth confined to adjacent neural structures without the direct involvement of visual pathway axons⁽⁸⁾.

To hasten the diagnosis of brain tumors in children, a consensus statement from 120 health care providers and parents presented several recommendations related to timely diagnosis. Initial management should include imaging after 2 weeks of persistent visual changes⁽³⁰⁾.

Table 4. Summary of studies on visual abnormalities in children with brain tumors, including findings from the current study

Author, year, and location	N	Age range (years)	Tumor location	Visual abnormalities at diagnosis
Wisoff et al., 1990, USA ⁽²³⁾	16	0.2-21.0	Supratentorial, midline, and infratentorial	LVA (n=11) VF loss (n=6) Strabismus/nystagmus (n=4)
Suharwardy & Elston, 1997, UK ⁽²²⁾	17 (12 boys)	1.0-13.0	Supratentorial, midline, and infratentorial	LVA (n=16) VF loss (n=9) Optic disc atrophy (n=7) Papilledema (n=4) Swollen disc (n=3) Disc pallor (n=2) Afferent pupillary defect (n=9) Proptosis (n=3)
Grabenbauer et al., 2000, Germany ⁽²⁰⁾	25 (14 boys)	1.5-16.0	Optic pathway	Visual disturbances (n=17) Strabismus (n=5) VF deficits (n=20)
Baroncini et al., 2007, France ⁽²¹⁾	16 (9 girls)	2.4-14.9	Thalamic	Visual dysfunction (n=7)
Crawford et al., 2007, USA ⁽²⁴⁾	30 (21 boys)	6.0-17.0	Supratentorial, midline, and infratentorial	LVA (n=13) Suprasellar: bitemporal hemianopsia (n=4) Pineal: 1 upgaze paralysis (Parinaud syndrome) Disseminated: mixed VF defects (n=1)
Santamaría, 2008, Spain ⁽²⁵⁾	58	<14.0	Supratentorial, midline, and infratentorial	Papilledema (n=17) Optic atrophy (n=14) Nystagmus VF loss Pupillary alterations (n=18) Dyschromatopsia (n=4) Amaurosis (n=3); Legal blindness (n=3)
Wilne et al., 2011, UK ⁽¹⁾	139 (82 boys)	0.8-16.7	Supratentorial, midline, and infratentorial	Papilledema (n=50) Nystagmus (n=25) Reduced visual acuity (n=20) Squint (n=18) Diplopia (n=18)
Pillai et al., 2012, Canada ⁽⁷⁾	35 (18 boys)	0.0-1.0	Supratentorial, infratentorial	Sunset eyes (n=21) Nystagmus (n=3)
Ghods et al., 2015, Iran ⁽²⁶⁾	(20 boys)	-1.0	Supratentorial (n=11) Infratentorial (n=6)	Supratentorial: sunset eyes (n=2), nystagmus (n=2), visual loss/no pursuit (n=2), ptosis (n=1) Infratentorial: sunset eyes (n=5), abducens nerve palsy (n=3)
Hoffmann et al., 2015, Germany ⁽²⁷⁾	411	0.0-9.0	Sellar/suprasellar	Visual impairment (n=161) Papilledema Optic atrophy
Alswaina et al., 2015, Saudi Arabia ⁽²⁾	26 (14 boys)	0.1-17.0	Supratentorial, midline, and infratentorial	LVA with disc pallor (n=10) LVA with disc swelling (n=3) Acquired strabismus with disc pallor or swelling (n=4) Acquired esotropia with diplopia (n=3) Acquired exotropia (n=4) Nystagmus (n=3)
Sánchez-Sánchez et al., 2016, Mexico ⁽²⁸⁾	51 (28 boys)	0.0-15.0	Supratentorial (n=19) Infratentorial (n=32)	Nystagmus (n=6 ST) Double vision (n=2 ST + 3 IT) LVA (n=4 ST) Strabismus (n=2 ST) Papilledema (n=1 ST + 1 IT)
Stocco et al., 2017, Italy ⁽²⁹⁾	75 (45 boys)	3.3-11.7	Supratentorial, midline, and infratentorial	Strabismus (n=16) Abnormal optic disc (n=11) Nystagmus (n=11) Double vision (n=9) Papilledema (n=8) Visual field defects (n=7) Palpebral ptosis (n=6) Anisocoria (n=4) Abnormal pupillary light reflex (n=3) Blurred vision (n=3) “Eyes wide open” episodes (n=3) Loss of stereopsis (n=1) Abnormal eye movements (n=1) Sunset eyes (n=1) Visual loss (n=1)
Dotto et al., 2020, Brazil ⁽⁶⁾	25 (13 boys)	0.2-7.9	Supratentorial/midline	Abnormal grating acuity (n=25) Nystagmus (n=17) Enlarged IAD (n=16) Abnormal optic nerve (n=13) Strabismus (n=12) Abnormal visual behavior (n=9)

IAD= interocular acuity difference; IT= infratentorial; LVA= low visual acuity; ST= supratentorial; VF= visual field.

Subsequent evaluation of visual function by SVEP would be extremely relevant to detect visual deficits in uncooperative, preverbal, and nonverbal children suspected of having a brain tumor.

In conclusion, in children with optic pathway tumors who are unable to perform recognition acuity tests, it is possible to detect and quantify visual impairment by objective grating acuity measurement. Detection of grating VA deficits complements clinical investigation and supports the neuro-oncologic management of these conditions.

ACKNOWLEDGMENTS

This study was financed in part by the Coordenação de Aperfeiçoamento de Pessoal de Nível Superior - Brasil (CAPES) - Finance Code 001.

REFERENCES

1. Wilne S, Collier J, Kennedy C, Jenkins A, Grout J, Mackie S, et al. Progression from first symptom to diagnosis in childhood brain tumours. *Eur J Pediatr*. 2012;171(1):87-93.
2. Alswaina N, Elkhamary SM, Shammari MA, Khan AO. Ophthalmic features of outpatient children diagnosed with intracranial space-occupying lesions by ophthalmologists. *Middle East Afr J Ophthalmol*. 2015;22(3):327-30.
3. Ostrom QT, Gittleman H, Liao P, Vecchione-Koval T, Wolinsky Y, Kruchko C, et al. CBTRUS Statistical Report: primary brain and other central nervous system tumors diagnosed in the United States in 2010-2014. *Neuro-oncol*. 2017;19 Suppl_5:v1-88.
4. Xu J, Margol A, Asgharzadeh S, Erdreich-Epstein A. Pediatric brain tumor cell lines. *J Cell Biochem*. 2015;116(2):218-24.
5. Dotto PF, Berezovsky A, Cappellano AM, da Silva NS, Sacai PY, Silva FA, et al. Visual function assessed by visually evoked potentials in optic pathway low-grade gliomas with and without neurofibromatosis type 1. *Doc Ophthalmol*. 2018;136(3):177-89.
6. Shofty B, Ben-Sira L, Kesler A, Constantini S. Optic pathway gliomas. *Adv Tech Stand Neurosurg*. 2015;42:123-46.
7. Pillai S, Metrie M, Dunham C, Sargent M, Hukin J, Steinbok P. Intracranial tumors in infants: long-term functional outcome, survival, and its predictors. *Childs Nerv Syst*. 2012;28(4):547-55.
8. Jariyakosol S, Peragallo JH. The effects of primary brain tumors on vision and quality of life in pediatric patients. *Semin Neurol*. 2015;35(5):587-98.
9. Wilne S, Collier J, Kennedy C, Koller K, Grundy R, Walker D. Presentation of childhood CNS tumours: a systematic review and meta-analysis. *Lancet Oncol*. 2007;8(8):685-95.
10. Kromer R, Serbecic N, Krastel H, Beutelspacher SC. Comparison of VEP with contrast sensitivity and other measurements of central visual function. *Acta Ophthalmol*. 2014;92(2):e141-6.
11. Trisciuzzi MT, Riccardi R, Piccardi M, Iarossi G, Buzzonetti L, Dickmann A, et al. A fast visual evoked potential method for functional assessment and follow-up of childhood optic gliomas. *Clin Neurophysiol*. 2004;115(1):217-26.
12. Salomão SR, Ventura DF. Large sample population age norms for visual acuities obtained with Vistech-Teller Acuity Cards. *Invest Ophthalmol Vis Sci*. 1995;36(3):657-70.
13. Salomão SR, Eizenbaum F, Berezovsky A, Sacai PY, Pereira JM. Age norms for monocular grating acuity measured by sweep-VEP in the first three years of age. *Arq Bras Oftalmol*. 2008;71(4):475-9.
14. Norcia AM, Tyler CW. Spatial frequency sweep VEP: visual acuity during the first year of life. *Vision Res*. 1985;25(10):1399-408.
15. de Freitas Dotto P, Cavascan NN, Berezovsky A, Sacai PY, Rocha DM, Pereira JM, et al. Sweep visually evoked potentials and visual findings in children with West syndrome. *Eur J Paediatr Neurol*. 2014;18(2):201-10.
16. Cavascan NN, Salomão SR, Sacai PY, Pereira JM, Rocha DM, Berezovsky A. Contributing factors to VEP grating acuity deficit and inter-ocular acuity difference in children with cerebral visual impairment. *Doc Ophthalmol*. 2014;128(2):91-9.
17. Chang BC, Mirabella G, Yagev R, Banh M, Mezer E, Parkin PC, et al. Screening and diagnosis of optic pathway gliomas in children with neurofibromatosis type 1 by using sweep visual evoked potentials. *Invest Ophthalmol Vis Sci*. 2007;48(6):2895-902.
18. Avery RA, Bouffet E, Packer RJ, Reginald A. Feasibility and comparison of visual acuity testing methods in children with neurofibromatosis type 1 and/or optic pathway gliomas. *Invest Ophthalmol Vis Sci*. 2013;54(2):1034-8.
19. Louis DN, Perry A, Reifenberger G, von Deimling A, Figarella-Braner D, Cavenee WK, et al. The 2016 World Health Organization classification of tumors of the central nervous system: a summary. *Acta Neuropathol*. 2016;131(6):803-20.
20. Grabenbauer GG, Schuchardt U, Buchfelder M, Rödel CM, Gusek G, Marx M, et al. Radiation therapy of optico-hypothalamic gliomas (OHG) – radiographic response, vision and late toxicity. *Radiother Oncol*. 2000;54(3):239-45.
21. Baroncini M, Vinchon M, Minéo JF, Pichon F, Francke JP, Dhellemmes P. Surgical resection of thalamic tumors in children: approaches and clinical results. *Childs Nerv Syst*. 2007;23(7):753-60.
22. Suharwardy J, Elston J. The clinical presentation of children with tumours affecting the anterior visual pathways. *Eye (Lond)*. 1997;11(Pt 6):838-44.
23. Wisoff JH, Abbott R, Epstein F. Surgical management of exophytic chiasmatic-hypothalamic tumors of childhood. *J Neurosurg*. 1990;73(5):661-7.
24. Crawford JR, Santi MR, Vezina G, Myseros JS, Keating RF, LaFond DA, et al. CNS germ cell tumor (CNSGCT) of childhood: presentation and delayed diagnosis. *Neurology*. 2007;68(20):1668-73.
25. Santamaría A, Martínez R, Astigarraga I, Etxebarria J, Sánchez M. [Ophthalmological findings in pediatric brain neoplasms: 58 cases]. *Arch Soc Esp Oftalmol*. 2008;83(8):471-7. Spanish.
26. Ghodsi SM, Habibi Z, Hanaei S, Moradi E, Nejat F. Brain tumors in infants. *J Pediatr Neurosci*. 2015;10(4):335-40.
27. Hoffmann A, Boekhoff S, Gebhardt U, Sterkenburg AS, Daubenbüchel AM, Eveslage M, et al. History before diagnosis in childhood craniopharyngioma: associations with initial presentation and long-term prognosis. *Eur J Endocrinol*. 2015;173(6):853-62.
28. Sánchez-Sánchez LM, Vázquez-Moreno J, Heredia-Delgado JA, Sevilla-Castillo R. Presentación clínica de tumores intracraneales supratentoriales (ST) e infratentoriales (IT) en pacientes pediátricos. *Gac Med Mex*. 2016;152(2):158-62.
29. Stocco C, Pilotto C, Passone E, Nocerino A, Tosolini R, Pusiol A, et al. Presentation and symptom interval in children with central nervous system tumors. A single-center experience. *Childs Nerv Syst*. 2017;33(12):2109-16.
30. Goldman RD, Cheng S, Cochrane DD. Improving diagnosis of pediatric central nervous system tumours: aiming for early detection. *CMAJ*. 2017;189(12):E459-63.